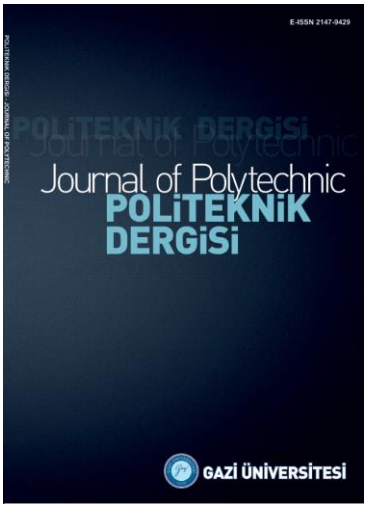

POLİTEKNİK DERGİSİ

JOURNAL of POLYTECHNIC

ISSN: 1302-0900 (PRINT), ISSN: 2147-9429 (ONLINE)
URL: http://dergipark.org.tr/politeknik

Viscoelastic characterization and mechanical hystheresis of commercial grade polypropylene

Ticari polipropilenin viskoelastik karakterizasyonu ve mekanik histerezis davranışı

Yazar(lar) (Author(s)): *Mustafa Mert YILMAZYURT[1], Serhat EYÜPREİSOĞLU[2], Ali Fethi OKYAR[3], Onur Cem NAMLI[4]*

ORCID[1]: 0000-0003-1697-6756

ORCID[2]: 0000-0002-1456-9359

ORCID[3]: 0000-0002-2561-7547

ORCID[4]: 0000-0003-3610-1914

To cite to this article: Yılmazyurt M. M., Eyüpreisoğlu S., Okyar A. F., Namlı O. C., "Viscoelastic characterization and mechanical hystheresis of commercial grade polypropylene" , ***Journal of Polytechnic***, 26(3): 1121-1130, (2023).

Bu makaleye şu şekilde atıfta bulunabilirsiniz: Yılmazyurt M. M., Eyüpreisoğlu S., Okyar A. F., Namlı O. C., "Viscoelastic characterization and mechanical hystheresis of commercial grade polypropylene" , ***Politeknik Dergisi***, 26(3): 1121-1130, (2023).

Erişim linki (To link to this article): http://dergipark.org.tr/politeknik/archive

DOI: **10.2339/politeknik.904719**

Viscoelastic Characterization and Mechanical Hysteresis of Commercial Grade Polypropylene

Highlights

- *Resolution of hysteresis response based on the computational viscoelasticity model*
- *Fitting of generalized Maxwell model parameters to experimental relaxation curves*
- *Determination of material behavior for commercial-grade materials without adequate specification*

Graphical Abstract

In this study, an analytical viscoelasticity model was determined to validate the material properties from the experimental response behavior. These results were compared with a finite element model to evaluate the results.

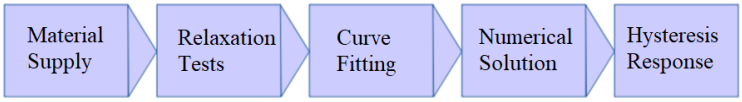

Figure. Diagram summarizing the study

Aim

This study aims to underline viscoelastic material properties of importance in the mechanical design process and provide a guideline to estimate them using a simple and easy characterization test.

Design & Methodology

The design of this study is based on the determination of a feasible analytical viscoelasticity model. This model is then used by way of experiments to determine and validate the viscoelastic material properties from experimental response curves. Finally, a numerical model is used to obtain further insight into the viscoelastic response.

Originality

This rationale behind our study stems from the lack of viscoelastic modeling in the mechanical design process involving the class of viscoelastic materials. Thus, we aimed to provide a fresh, original, and simple method for mechanical engineers.

Findings

The viscoelastic response of an off-the-shelf stock polypropylene material was determined by fitting the experimental response curves by an appropriate viscoelastic material model.

Conclusion

Although the undertaking of a viscoelastic response analysis is comparably more involved than that of an elastic material class, there will be significant advantages and insights provided by the viscoelastic model which will be useful in making design decisions.

Declaration of Ethical Standards

The authors of this article declare that the materials and methods used in this study do not require ethical committee permission and/or legal-special permission.

Viscoelastic Characterization and Mechanical Hysteresis of Commercial Grade Polypropylene

Araştırma Makalesi/Research Article

Mustafa Mert YILMAZYURT, Serhat EYÜPREİSOĞLU, Ali Fethi OKYAR, Onur Cem NAMLI

Faculty of Engineering, Mechanical Engineering Department, Yeditepe University, Istanbul, Turkey

(Geliş/Received : 29.03.2021 ; Kabul/Accepted : 25.02.2022 ; Erken Görünüm/Early View : 27.03.2022)

ABSTRACT

The main objective of this project is to investigate the viscoelastic behavior of polypropylene material. The theory of viscoelasticity is used to understand how a polypropylene material can be modeled mathematically to make a complete analysis. The time-dependent stress-strain response of the polypropylene material is investigated with the relaxation test that is carried out with the material. Then the required parameters for mathematical models such as elasticity or stiffness, k or E, along with the relaxation time, $\boldsymbol{\tau}$, is found to illustrate this behavior. The response curve from experiments is compared with the analytical study with the theory that includes the mathematical models to complete a finite element analysis on Marc. The curve that is achieved from this analysis overlapped with the one coming from the analytical study. Forced oscillation procedure is carried out in Marc to simulate the dynamic analysis test. Internal energy loss of the specimen is inspected via the hysteresis graph.

Keywords: Viscoelasticity, finite element method, relaxation modulus, collocation method, hysteresis.

ÖZ

Bu projenin temel amacı, bir polipropilen malzemenin viskoelastik davranışını incelemektir. Viskoelastisite teorisi, tam bir analiz yapmak için bir polipropilen malzemenin matematiksel olarak nasıl modellenebileceğini anlamak için kullanılır. Polipropilen malzemenin zamana bağlı gerilme-uzama tepkisi, malzeme ile yapılan gevşeme testi ile araştırılır. Daha sonra esneklik veya sertlik gibi matematiksel modeller için gerekli parametreler, k veya E, gevşeme süresi ile birlikte, $\boldsymbol{\tau}$, bu davranışı göstermektedir. Deneylerden gelen yanıt eğrisi, Marc yazılımı üzerinde bir sonlu eleman analizini tamamlamak için matematiksel modelleri içeren teori ile analitik çalışma ile karşılaştırılmıştır. Bu analizden elde edilen eğri, analitik çalışmadan gelenle örtüşmektedir. Dinamik analiz testini simüle etmek için Marc'ta zorunlu salınım prosedürü gerçekleştirilmiş ve numunenin dahili enerji kaybı histerezis grafiği ile incelenmiştir.

Anahtar Kelimeler: Viskoelastisite, sonlu elemanlar yöntemi, gevşeme modülü, kolokasyon yöntemi, histerezis

1. INTRODUCTION

Plastic materials are one of the worst pollutants in the worlds' oceans, due to their ubiquitous use in daily life as well as industrial applications, which are too great to list here [1]. It is important to recycle plastics to mitigate the pollution caused by them. Recycling, however, alters the mechanical properties of the original constituents by mixing them with others, thus an in-situ material characterization just after the recycled product is obtained becomes important. In this way, recycled products which come with their material property specifications may readily be integrated into the engineering design cycle [2], which in turn will increase the utilization of recycled plastics in the industry.

One of the most common types of plastic in daily-life use is polypropylene (PP), most of the plastic kitchen appliances such as food storage boxes, plastic cutting boards, plastic glasses are made of this material, and filters of water purification devices consist of a body and a cover part made of PP material [3]. Although PP in room temperature may be assumed to behave as a linearly elastic material for brevity in engineering design, a more detailed analysis will require knowledge about its viscoelastic properties, which usually is missing from the manufacturer's specifications. Energy absorption capacity [4] and mechanical properties of recycled plastic materials [5] are recent studies done on plastics and polymers. In this study, a PP material without any knowledge of composition or material properties was purchased off-the-shelf of a Turkish supermarket chain to characterize its' viscoelastic behavior.

Viscoelasticity is a mechanical phenomenon that differs from elasticity by including the temporal behavior of the material [6], [7]. While elastic materials respond instantaneously to an externally applied load or displacement and keep their shape as time lapses, viscoelastic materials keep deforming or changing their internal loads with time. Thus the mathematical theory of viscoelasticity may get quite complex in comparison with the theory of elasticity. In this study, we aimed to keep the mathematical complexity of the viscoelastic formulation at the lowest level yet achieve a sufficient experimental fit of the analytical parameters. This aim was satisfied by using the generalized Maxwell model. The viscoelastic behavior of PP has been studied experimentally by [8], however, they did not consider using a generalized Maxwell model.

**Sorumlu Yazar (Corresponding Author)*
e-posta : onur.namli@yeditepe.edu.tr

In the experiments, the test specimens were cut from stock, and numerous stress relaxation tests were made at different conditions. Based on fitting these curves with various viscoelastic models, material parameters have been estimated. The specimen used in the tests was also modeled in the finite element software MARC, [6] by using a viscoelastic material model and the material parameters obtained in the previous step. Using appropriate loading and boundary conditions, the stress relaxation behavior of the numerical model was obtained and then compared with the analytical model. Moreover, the numerical model provided an extra insight that was otherwise not available, that is the stress-strain behavior of the PP material. Viscoelasticity is seldom exploited in the mechanical design process. The main objective of this article is to propose a simple experimental layout for the in-situ measurement of viscoelastic parameters of recycled plastics. In addition, we showed the hysteresis of PP material as a bi-product of the computational results, which is often a concept left out of the design process.

2. LINEAR VISCOELASTIC THEORY

2.1. THE MAXWELL MODEL

The mechanical response of a viscoelastic material under external stress exhibits both the characteristics of an elastic solid as well as a viscous fluid. In addition, it is known that springs and dashpots are devices that exhibit elastic and viscous responses, respectively. Thus, the equations relating to stress and strain of a viscoelastic material could be represented with an appropriate combination of equations that relate stress and strain as in springs and dashpots. To illustrate, these spring dashpot systems utilize a Hookean model spring described by,

$$\sigma_s = k\varepsilon \tag{1}$$

where σ_s and ε are the uniaxial stress and strain analogous with the spring force and the displacement, respectively, and the spring constant k is analogous with Young's modulus E (The stiffness, k, will be used interchangeably with E in the remaining parts of the paper). While the instantaneous deformation of the materials is modeled as a spring, its fluid-like flow can be modeled using a Newtonian dashpot for which stress and strain rates are related as

$$\sigma_d = \eta\dot{\varepsilon} \tag{2}$$

where η is the viscosity ($N - s/m^2$). Taking the ratio of viscosity to stiffness as

$$\tau = \eta/k \tag{3}$$

the time of viscoelastic response or viscoelastic time constant of the material τ is obtained.

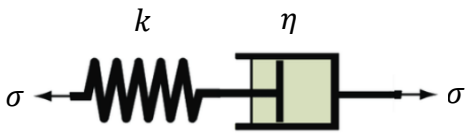

Figure 1. The Maxwell Model

The model shown in Figure 1 known as the Maxwell model is a series assembly of the spring and dashpot. In this model, the stress in each element is the same as the applied stress while a strain is obtained by summing strains over the respective components.

$$\sigma = \sigma_s = \sigma_d \tag{4}$$

$$\varepsilon = \varepsilon_s + \varepsilon_d \tag{5}$$

Here, the subscripts *d* and *s* represent dashpot and spring respectively. If Eqs. 2 and 3 are combined with Eq. 5, we get

$$\varepsilon = \dot{\varepsilon}_s + \dot{\varepsilon}_d = \frac{\dot{\sigma}}{k} + \frac{\sigma}{\eta} \tag{6}$$

Multiplying the above with *k*, and inserting the time constant from Eq. 3 we get

$$k\dot{\varepsilon} = \dot{\sigma} + \left(\frac{1}{\eta}\right)\sigma \tag{7}$$

The left-hand side of the above equation disappears when the material is placed in a relaxation test where the applied strain remains constant throughout the test. The applied strain and relaxation stress versus time graphs are as seen in Figure 2.

Upon substituting $\dot{\varepsilon} = 0$ into Eq. 7 we get

$$\dot{\sigma} = -\left(\frac{1}{\tau}\right)\sigma \tag{8}$$

Using separation of variables and integrating both sides,

$$\int_{\sigma_0}^{\sigma} \frac{d\sigma}{\sigma} = -\left(\frac{1}{\tau}\right)\int_0^t dt \tag{9}$$

$$\log\sigma - \log\sigma_0 = -\frac{t}{\tau} \tag{10}$$

$$\sigma(t) = \sigma_0 \exp\left(-\frac{t}{\tau}\right) \tag{11}$$

Normalizing Eq. 11 with respect to the applied strain, ε_0, we obtain the relaxation modulus E_{rel}

$$E_{rel}(t) = \frac{\sigma(t)}{\varepsilon_0} = k\exp\left(-\frac{t}{\tau}\right) \tag{12}$$

Where Eq. 1 was used.

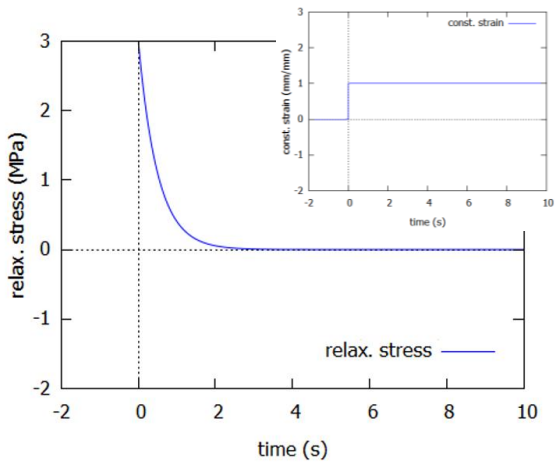

Figure 2. Constant strain and Resulting stress curve vs. time (s).

2.2. THE STANDARD LINEAR SOLID (SLS) MODEL

Plastic materials or polymers do not show the relaxation behavior exhibited by the Maxwell model shown in Figure 2 unless they are silly putty. Different differentiated spring-dashpot models can be used to illustrate the reorganization of conformational shape that occurs within the material. For example, the Standard Linear Solid (SLS) Model shown in Figure 3, is obtained by placing one more spring, k_e, parallel to the Maxwell model explained in the previous part. This spring provides a rubbery stiffness when Maxwell side is relaxed away during dashpot extension.

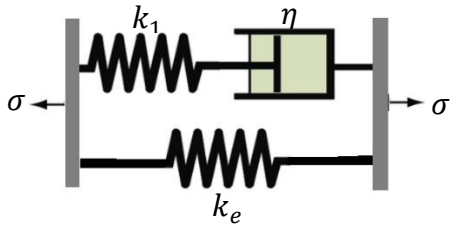

Figure 3. The Standard Linear Solid (SLS) Model

Eventually, there will be the same strain (iso-strain) occurring on both sides of the model.

$$\varepsilon = \varepsilon_e = \varepsilon_m \tag{13}$$

Total stress will be the sum of both sides.

$$\sigma = \sigma_e + \sigma_m \tag{14}$$

As Maxwell part of the model contains the stress and the stress is dependent on time, it can be solved with Laplace transformation easily. Also SLS model contains one more spring alongside the Maxwell Model the Eq. 7 converts to;

$$k_1\dot{\varepsilon} = \dot{\sigma}_m + \left(\frac{1}{\tau}\right)\sigma_m \tag{15}$$

If Laplace transformation is applied,

$$k_1 s\bar{\varepsilon} = s\bar{\sigma}_m + (1/\tau)\bar{\sigma}_m \tag{16}$$

and σ_m is isolated,

$$\bar{\sigma}_m = \frac{k_1 s}{s + (1/\tau)}\bar{\varepsilon} \tag{17}$$

Upon adding the stress contribution from the parallel Maxwell element,

$$\bar{\sigma} = k_e\bar{\varepsilon} + \frac{k_1 s}{s + (1/\tau)}\bar{\varepsilon} = \left(k_e + \frac{k_1 s}{s + (1/\tau)}\right)\bar{\varepsilon} \tag{18}$$

As in the Hooke's Law, the Eq. 18 is simplified to $\bar{\sigma}=E\bar{\varepsilon}$ where the E is called the relaxation modulus in the frequency domain, which reads,

$$E = k_e + \frac{k_1 s}{s + (1/\tau)} \tag{19}$$

For example, if a constant strain ε_0 is applied to the material as discussed earlier in Figure 2, one can expect $\varepsilon(t) = \varepsilon_0$, and it's Laplace transform reads

$$\bar{\varepsilon} = \frac{\varepsilon_0}{s} \tag{20}$$

Upon dividing Eq. 18 by ε_0, and taking the inverse Laplace transform, one can get

$$E_{rel}(t) = \frac{\sigma(t)}{\varepsilon_0} = k_e + k_1 \exp\left(-\frac{t}{\tau}\right) \tag{21}$$

The SLS model is a model with three parameters, k_e glassy moduli, k_1 rubbery moduli and τ is the relaxation time.

$$k_e = E_r \tag{22}$$

$$k_1 = E_g - E_r \tag{23}$$

$$\tau = t@E_{rel} = E_r + \frac{1}{e}(E_g - E_r) \tag{24}$$

2.3. THE WIECHERT MODEL

In reality, the SLS model is not sufficient in capturing the viscoelastic relaxation behavior of PP, where, one can observe a relaxation with a distribution of relaxation times due to the variation of molecular bonds occurring. As there is a change in the length with more number of shorter-parts relaxing quicker than the longer ones, the relaxation process expands over a longer time than usual. Thus, there will be more elements needed to model this phenomenon, and the Wiechert model also known as the Prony series model addresses this need. There are some studies made through years comparing the Wiechert Model to the previously discussed SLS Model [10] [11] [12].

$$\sigma = \sigma_e + \sum_j \sigma_j \tag{25}$$

The illustration of the $j + 1$ armed Wiechert model can be seen in Figure 4.

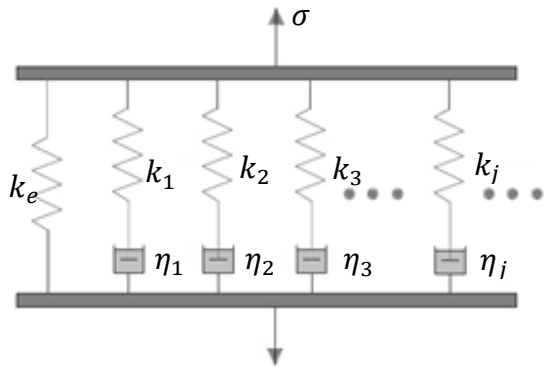

Figure 4. The Wiechert Model

The total stress σ is the algebraic combination of the equilibrium spring and remaining j the Maxwell arms. Using Eq. 3 the formula for each Maxwell arms can be written as,

$$\bar{\sigma}_j = \frac{k_j s}{s + (1/\tau_j)}\bar{\varepsilon} \tag{26}$$

The Laplace transformed formula of the model will be

$$\mathrm{E} = k_e + \sum_j \frac{k_j s}{s + (1/\tau_j)} \tag{27}$$

$$\bar{\sigma} = \bar{\sigma}_e + \sum_j \bar{\sigma}_j = \left(k_e + \sum_j \frac{k_j s}{s + (1/\tau_j)} \right)\bar{\varepsilon} \tag{28}$$

If there is a constant strain ε_0 applied to the material as discussed for the Maxwell spring-dashpot model, the stress can be calculated as,

$$\begin{aligned} \bar{\sigma}(s) = \bar{\mathrm{E}}(s)\bar{\varepsilon}(s) &= \left(k_e + \sum_j \frac{k_j s}{s + (1/\tau_j)} \right)\frac{\varepsilon_0}{s} \\ &= \left(\frac{k_e}{s} + \sum_j \frac{k_j}{s + (1/\tau_j)} \right)\varepsilon_0 \end{aligned} \tag{29}$$

$$\sigma(t) = \mathcal{L}^{-1}[\bar{\sigma}(s)] = \left(k_e + \sum_j k_j \exp\left(-t/\tau_j\right) \right)\varepsilon_0 \tag{30}$$

Normalizing with ε_0, the relaxation modulus E_{rel} can be found as;

$$E_{rel} = k_e + \sum_j k_j \exp\left(-t/\tau_j\right) \tag{31}$$

Such a viscoelastic material under dynamic loading dissipates energy at every cycle. The energy difference between the loading and unloading causes a loss of energy which emancipates in the form of dissipated heat from the material. The reason for the energy difference is explained by the phase lag between the applied load and the deformation obtained observed in the complex plane. It is useful to visualize the stress and strain as vectors rotating about the origin of the complex plane at a given angular speed, ω. Under applied stress, $\sigma(t)$, the strain, $\varepsilon(t)$ lags it by the phase angle δ as seen in Figure 5 where the lag between stress and strain oscillations and the rotating vector in the complex plane representing the lag in terms of angle δ are shown.

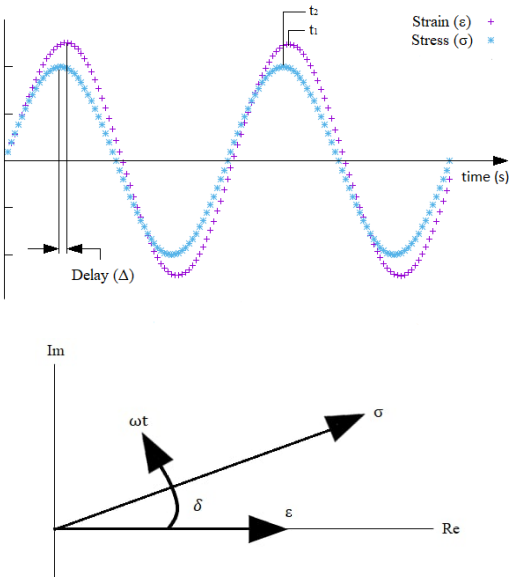

Figure 5. The lag between stress and strain oscillations (Top), Rotating Vector in the complex plane representing the lag in terms of angle δ (Bottom) [13].

The relations between the phase lag δ, real and imaginary parts of the stress σ_0' and σ_0'' are given in Eqs (32)-(35).

$$\tan\delta = \sigma_0''/\sigma_0' \tag{32}$$

$$|\sigma^*| = \sigma_0\sqrt{\sigma_0'^2 + \sigma_0''^2} \tag{33}$$

$$\sigma_0' = \sigma_0\cos\delta \tag{34}$$

$$\sigma_0'' = \sigma_0\sin\delta \tag{35}$$

The complex form of the stress function can be used to describe two different dynamic parameters [4], known as the storage modulus, E', and the loss modulus, E'', which are represented as

$$E' = \sigma_0'/\varepsilon_0 \tag{36}$$

$$E'' = \sigma_0''/\varepsilon_0 \tag{37}$$

Dynamic tests are suitable for understanding short-term polymer responses. When a viscoelastic material is subjected to sinusoidal varying stress, a steady-state condition will be reached where the resulting species (output) is also sinusoidal, with the same angular frequency but is delayed by an angle δ in phase, while the delay in the time is shown by Δ. The time lag $\Delta = t_2 - t_1$ is the difference between the peaks of strain and stress responses as shown in Figure 5. The phase lag δ and time lag δ are related to each other by the following Eqs. 38-39.

$$2\pi f t_2 = 2\pi f t_1 + \delta \tag{38}$$

$$\delta = 2\pi\Delta/\lambda \tag{39}$$

Here, f is the frequency of loading inversely proportional to the wavelength, λ. The delay between stress and strain is plotted for different frequency values. For frequency values less than 1 Hz, the delay is expected to increase as the frequency value decreases. As the frequency values increase, the delay occurring is expected to decrease and reset after a while.

3. EXPERIMENTAL METHOD

The model parameters k_e, $k_1 \dots k_j$ and $\tau_1 \dots \tau_j$ can be found by data fitting methods if relaxation tests are provided. For this purpose, several such tests are performed in the uniaxial testing machine where the change in stress was recorded over prolonged periods of exposure at a constant elevated temperature. Several tests were performed at room temperature and at higher temperatures which are generated by a heat gun. The results were then compared with the ones in the literature.

Relaxation tests in the study were made with a universal testing machine (Instron 3382) located in the Solid Mechanics Laboratory at Yeditepe University Mechanical Engineering Department. A constant strain ε_0 was applied to the tensile test coupon made of PP material and it was kept constant while the load was recorded with respect to time. The engineering stress variation was generated with the help of loading data. A constant elongation was introduced to the test coupon in the form of a ramp function but the rise time was kept as small as possible to approximate a Heaviside step function. The instantaneous relaxation modulus is calculated by

$$E_{rel}(t) = \frac{\sigma(t)}{\varepsilon_0} \tag{40}$$

Figure 6. Test coupon inside Instron machine (Left) and the machine with a heat gun pointing at the coupon (Right)

Several relaxation tests were performed at three different temperatures. In each, the ramp time was set to be 1 second but data acquisition frequency was varied according to the total experiment time [14]. Initial experiments were done at room temperature whereas other ones at elevated temperatures were generated by a heat gun to accelerate the process of relaxation. The temperature of the test coupon subjected to heating was recorded by an infrared thermometer.

For materials that are considered as thermo-rheologically simple, if the operating temperature decreases, then, the viscoelastic response will be shifted to the right side of the relaxation graph in Figure 2 without changing the shape of the curve. This effect also corresponds to an increase in relaxation time in Eq. 21. The glassy and the rubbery moduli do not change as well. We introduce a time-temperature shift factor, $a_T(T)$ to horizontally shift the curve from an arbitrary temperature [15]. Upon repeating this procedure at different temperatures a master curve is generated using the formula,

$$\log(a_T) = \log \tau(T) - \log \tau(T_{ref}) = \log \tau(T/T_{ref}) \tag{41}$$

Data Fitting

Fitting of the viscoelastic model parameter to experimental data has been undertaken in previous studies [11] [12] [16]. One of the most popular numerical methods for data fitting in relaxation tests was seen to be the collocation method [11] [12]. In this method the elastic stiffness parameters $E_0 \dots E_j$ are determined for a given choice of relaxation time parameter set $\tau_1 \dots \tau_j$ by solving a linear system of equations. Such a linear system for a 7-arm Wiechert model is shown in Eq. 42.

$$\begin{bmatrix} 1 & 1 & 1 & \dots & 1 \\ 1 & e^{-(\tau_1/\tau_1)} & e^{-(\tau_1/\tau_2)} & \dots & e^{-(\tau_1/\tau_6)} \\ 1 & e^{-(\tau_2/\tau_1)} & e^{-(\tau_2/\tau_2)} & \dots & e^{-(\tau_2/\tau_6)} \\ \vdots & \vdots & \vdots & \ddots & \vdots \\ 1 & e^{-(\tau_6/\tau_1)} & e^{-(\tau_6/\tau_2)} & \dots & e^{-(\tau_6/\tau_6)} \end{bmatrix} \begin{bmatrix} E_0 \\ E_1 \\ E_2 \\ \vdots \\ E_7 \end{bmatrix} = \begin{bmatrix} E_{rel}(0) \\ E_{rel}(\tau_1) \\ E_{rel}(\tau_2) \\ \vdots \\ E_{rel}(\tau_7) \end{bmatrix} \tag{42}$$

4. FINITE ELEMENT ANALYSIS

A simple finite element model of the uniaxial tensile test setup was built in the software called MARC. Then, it was solved according to suitable boundary and loading conditions. The geometry of the specimen was created and was converted into a mesh of finite elements in MARC. Then, properties were assigned for these elements using the viscoelastic material specification. After this process, the necessary boundary conditions were specified.

An 8-element rectangular model was used on the Marc software. The model is 45 mm long, 8.85 mm wide, and 6.6 mm high following the actual test specimen. The number of elements was kept at a minimum level as the expected stress distribution in the domain was uniform.

As seen in Figure 7, two meshes were created, one for the quasi-static relaxation test and the other one for the dynamic loading. The mesh defined for the dynamic loading used a relatively finer mesh structure to account

for longitudinal wave propagation within the specimen. A simple convergence analysis was carried out for the dynamic model to ensure sufficient accuracy in the numerical result has been achieved.

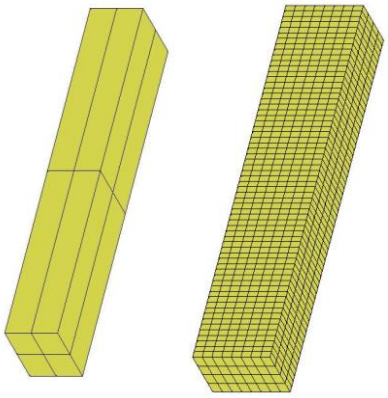

Figure 7. Mesh used for the quasi-static relaxation (Left), and the finer mesh used in dynamic loading (Right)

Boundary conditions were entered into the software according to the physical test. One end of the model was fixed. The other end was pulled 3 mm in the longitudinal direction. This pulling takes place in 1 second. Then, the model drawn 3 mm is held in this position and the stress relief in the model was observed.

Dynamic loading is introduced by specifying one end of the specimen fixed while the other end was subjected to a cyclic displacement. The loading pattern for a loading frequency of 2 Hz is shown in Figure 8.

Frequency values are gradually increased from 1 Hz to 1024 Hz. For this process, 128 and 1024 element models were used. Then the frequency value was gradually decreased from 1 Hz to 1/256 Hz. The model used here had 2048 elements.

4.1. MATERIAL SPECIFICATIONS

With the data obtained from the analytical and practical studies shear and bulk moduli, $G(t)$, and $K(t)$ were found for different relaxation time values. These values were added to the viscoelastic section which is a special tab in Marc. The material density is selected to be 0.855 g/cm³ for PP. In addition, Young's modulus value for the material is 450 MPa which is selected according to materials first response to relaxation test and Poisson's ratio is 0.43 in literature as well. Yet, this value can be found with a multi-axial test where the lateral contraction in a uniaxial tensile test is inspected [17].

The relaxation modulus $E(t)$ was determined from a 7-arm Wiechert model for which the stiffness parameters $k_0, \dots, k_6$ and time constants $\tau_0, \dots, \tau_6$ were supplied.

Then the following formulas were used and μ in the formulas represents the Poisson's ratio [18] [19].

$$G(t) = \frac{E(t)}{2(1+\mu)} \tag{43}$$

$$K(t) = \frac{E(t)}{3(1-2\mu)} \tag{44}$$

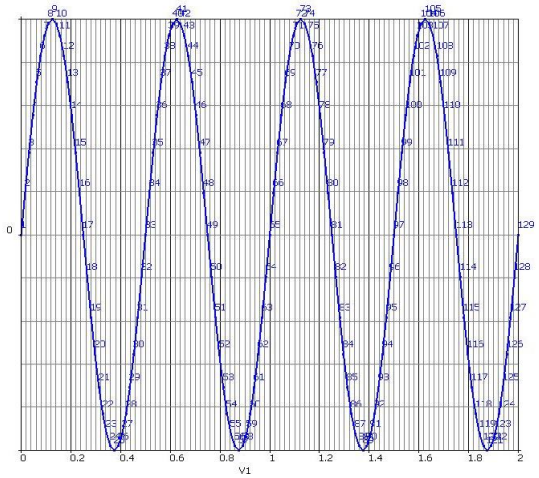

Figure 8. Marc Table Tab and Table for 2 Hz

5. RESULTS & DISCUSSION

5.1. STRESS RELAXATION

Seven relaxation curves were obtained in total. While Four of them were made at approximately room temperature, the other three coupons were heated with a heat gun to reach higher temperatures between 55 to 65 °C at a data collection rate of 100 Hz as seen in Figure 9.

Data collection rate, duration as well as the temperature of the specimen were varied to capture the glassy and viscous plateau as well as the transition region. The glassy modulus, E_g, was recorded as 450 MPa for the tests at room temperature, while it decreased to 270 and 180 MPa for the tests at 55 and 65 °C, respectively. Furthermore, the rubbery modulus E_r was recorded at approximately 50 MPa for the coupon heated to 65 °C. The relaxation modulus versus time behavior is in good agreement for tests conducted at different temperatures with the experimental results produced in [8]. Although the overall behavior is not as simple as expected from a thermo-rheologically simple material, the time-temperature shifting technique ([7]) was still found to be applicable to obtain an overall idea about the temporal relaxation behavior.

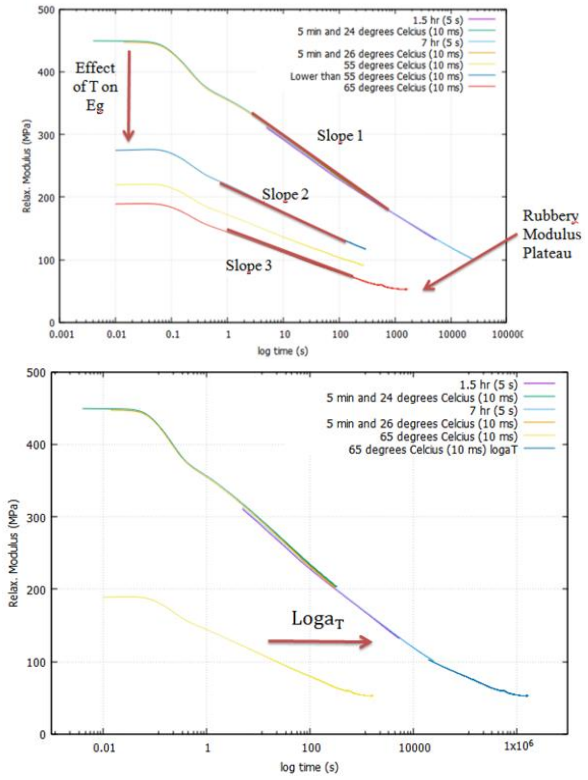

Figure 9. Relaxation test for various conditions such as temperature, and the rubbery plateau (Top), master curve generation from the relaxation test curves (Bottom)

After generating the master curve, a viscoelastic transition behavior from the glassy region (450 MPa) to the rubbery region (50 MPa) was found. Two different models were fitted to the master relaxation curve, namely the SLS model, and the Wiechert model having 7 arms. The SLS model was adjusted to fit between the glassy and rubbery plateau as seen in Figure 10. The fitting curve obtained with the SLS model was found to have a transition region of limited width in comparison with the experimentally obtained master curve.

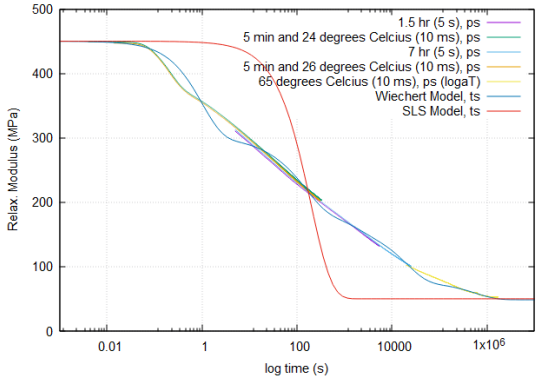

Figure 10. The fitting curve obtained with Wiechert & SLS Models

Upon applying the collocation procedure for a 7 arm Wiechert model, the stiffness values were found as can be seen in Table 1.

Table 1. Constants for Wiechert Model with 6 arms

No	E_{rel} (MPa)	τ(s)	E (N/mm)(calc.)
0	450	0	48.6
1	354	1	149.9
2	280	20	11.2
3	222	150	100.1
4	163	1500	31.4
5	105	2.0e+4	81.5
6	59	5.8e+5	27.3

Using the set of parameters given in Table 1 the Wiechert model curve is seen to be in good agreement with the master curve as shown in Figure 10 [20].

5.2. FINITE ELEMENT VALIDATION

The analytical and experimental results outlined above in the previous sections were complemented with numerical results obtained from MARC. A six-arm Wiechert material model has used parameters which are listed in Table 2.

Table 2. Shear and Bulk Moduli for the six-arm Wiechert model used in Marc

τ(s)	$G(t)$ (MPa)(calc.)	$K(t)$ (MPa)(calc.)
1	52.42	356.93
20	3.92	26.71
150	35.00	238.33
1500	10.88	74.12
2.0e+4	30.28	193.95

As seen in Figure 11, the analytical and numerical solutions (FEA) from the Marc program are in nearly exact agreement with each other.

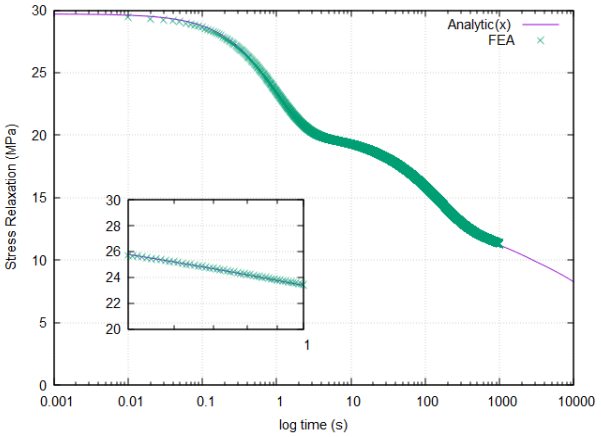

Figure 11. Relaxation Test Results

The curve represented by the purple line in Figure 11 represents the numerical solution, while the green dots on this purple curve show the results obtained from MARC.

The overlapping curves in this Figure 11 show that the numerical model has correctly been implemented.

5.3. DYNAMIC RESPONSE

The computational model setup in MARC was also subjected to cyclic displacements at one end while its other end was held fixed. The model was forcibly excited in this way under a considerable range of frequencies (0.01 – 100 Hz). The resulting stress and strain responses were recorded in time. It was observed that a phase difference between the stress and strain occurred but the phase had changed with the frequency of excitation. As an example, the stress and strain for 1/128 Hz values are shown in Figure 12. The delay between stress and strain can be observed in this figure.

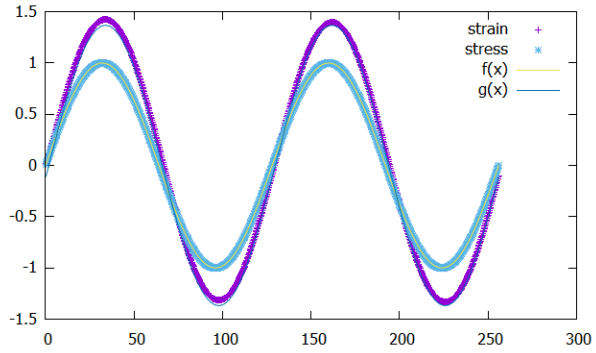

Figure 12. Stress and Strain for 1/128 Hz

Frequency values were gradually decreased starting from 1 Hz to 1/256 Hz, and stress-strain graphics of the results were created. In the same way, starting from 1 Hz to 1024 Hz, it was gradually increased and its results were recorded.

The stress and strain curves in Figure 12 were fitted with a sinusoidal function of the form $g(t) = a\sin(b + ft)$ where f denotes the excitation frequency and a and b are the fitting constants. The corresponding phase difference, δ is found by taking the difference of b from the stress and strain curves. Repeating the procedure for a range of frequencies in [0.01,100] Hz, we obtain the frequency response of the phase shift as shown in Figure 13 [21].

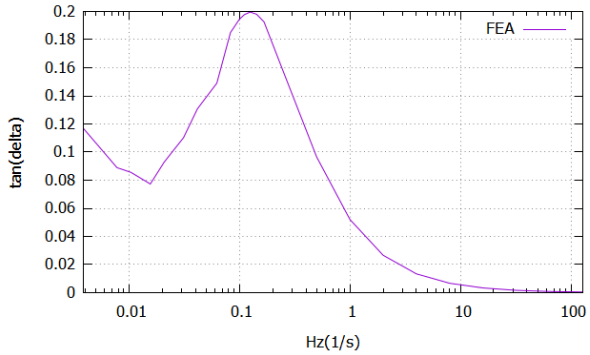

Figure 13. Tan δ vs. Frequency Graph

Figure 13 was created with a total of 27 frequency values, at high-frequency values, the delay between stress and strain is too little or zero. The peak of delay occurs in the range of 0.1 to 0.2 Hz.

5.4. HYSTERESIS

As the phase difference between stress and strain increases more energy is dissipated at each loading cycle. Figure 13 represents the high internal energy loss of material at frequency values where tan δ is high. The energy loss during each loading cycle may either be associated with dissipated heat from the body or molecular rearrangement within. In this case, it is seen in Figure 13 that the internal energy loss is high in the frequency range of 0.08 and 0.12 Hz. To better understand the energy loss there, it is good practice to create a hysteresis graph with a time-dependent stress-strain curve.

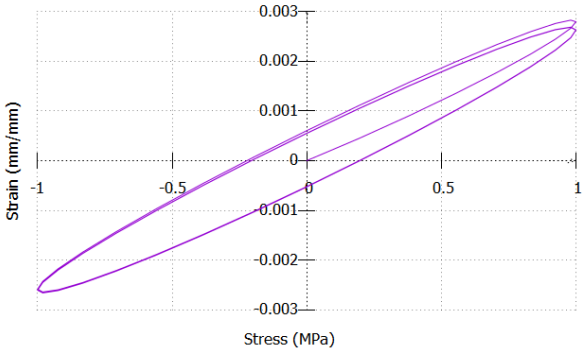

Figure 14. Hysteresis Graph

The hysteresis graph is obtained by plotting the stress/strain pairs at a given instant during the loading cycle onto the stress-strain diagram. As the time proceeds and more points are added a loading curve parametric in time appears on the graph. It is seen that the loading and unloading paths are not collinear thus the area enclosed by the curve can be identified as the energy loss density per cycle. For example, the hysteresis curve corresponding to a loading frequency of 1/7 Hz is shown in Figure 14. As the peak frequency values seen in Figure 13 are reached, this area in the middle will grow. This area, which is in the middle, will shrink as larger frequency values are reached [22].

For an elastic material, the energy provided to bring the material into different shapes is stored as potential energy inside. This energy is used to restore the original size and shape after the applied stress is removed. The loading and unloading curves are identical for an elastic material. This indicates that there is no energy loss during loading and unloading. For a viscoelastic material, things are slightly different. Some of the strain energy is stored inside as potential energy, while the other part is distributed as heat. It should be noted that most elastic materials exhibit dissipation at stress levels beyond the yield point.

For viscoelastic materials, some of the deformation energy is dissipated as heat during plastic deformations. The presence of the hysteresis cycle can be seen in their loading and unloading diagrams. Viscoelastic materials distribute energy regardless of whether the strains or stresses are small or large. Viscoelastic materials show time-dependent material behavior, so the differences between elastic and viscoelastic material responses are most evident under time-dependent loading conditions [23] [24].

6. CONCLUSION

Viscoelasticity is a branch of solid mechanics that awaits to be further exploited using modern experimental tools and computational software. It is more difficult to find manufacturer's specifications about viscoelastic materials, especially in our country and the number of academic papers in this area is quite low. For this reason, this study intends to inspire future academic studies in the field of recycled plastic materials [25]. The behavior of viscoelastic materials can be better interpreted with an increasing number of studies to be carried out on this area and an increased usage of these materials in engineering design can be expected.

Finite element software is a tool to create solutions to complex problems which can be very useful and save loads of time. In this study, the viscoelastic behavior of a PP material is examined by experimental studies made via an Instron machine, and the results were compared with analytical studies involving the Wiechert and SLS models. Finally, the same material was modeled in MARC.

DECLARATION OF ETHICAL STANDARDS

The authors of this article declare that the materials and methods used in this study do not require ethical committee permission and/or legal-special permission.

AUTHORS' CONTRIBUTIONS

Mustafa Mert YILMAZYURT: Took part in analytical and experimental studies and the association of these with each other.

Serhat EYÜPREİSOĞLU: Build the appropriate model on the Marc program, obtained the numerical test results, and compared them with previous test results. He modeled the forced oscillation experiment on the validated model in the Marc program and drew the results of the results.

Ali Fethi OKYAR: Supervised the graduation theses of Mustafa Mert Yılmazyurt (Fall 2019) and Serhat Eyüpreisoğlu on this subject, and led the conversion of their theses to this manuscript.

Onur Cem NAMLI: Took part in the stress relaxation testing and analysis of the viscoelasticity results and the association of these results with each other.

CONFLICT OF INTEREST

There is no conflict of interest in this study.

REFERENCES

[1] https://www.unep.org/interactive/beat-plastic-pollution/, United Nations Environment Programme, "Beat Plastic Pollution".

[2] G. Dieter and L. Schmidt, ***"Engineering Design"***, McGraw-Hill Book Company, (2021).

[3] H. Maden and K. Çetinkaya, "Joining analysis of polypropylene parts in the rotary friction welding process and developing of joints profile," ***Politeknik Dergisi***, 24(3):1263-1273, (2021).

[4] E. Yeter, "Investigation of ballistic impact response of aluminum alloys hybridized with kevlar/epoxy composites," ***Politeknik Dergisi***, 22(1): 219-227, (2019).

[5] A. Gültekin Toroslu, "Geri dönüşümlü Akrilonitril Bütadiyen Stiren (ABS) plastik malzemesinin kalıplama parametrelerine etkisi," ***Politeknik Dergisi***, 23(1): 1-6, (2020).

[6] D. Gutierrez-Lemini, ***"Engineering Viscoelasticity"***, Springer, Boston, U.S.A., (2014).

[7] http://web.mit.edu/course/3/3.11/www/modules/visco.pdf, D. Roylance, "Engineering Viscoelasticity", (2001).

[8] T. Ariyama, Y. Mori and K. Kaneko, "Tensile properties and stress relaxation of polypropylene at elevated temperatures," ***Polymer Engineering & Science***, 37(1): 81-90, (1997).

[9] MSC Software, "***Vol A: Theory and User Information"***, Santa Ana, U.S.A., (2018).

[10] J. Kim, J. Kyoung, A. Sablok, and K. Lambrakos, "A Nonlinear Viscoelastic Model for Polyester Mooring Line Analysis," ***Proceedings of the International Conference on Offshore Mechanics and Arctic Engineering - OMAE***, 1, (2011).

[11] C. Machiraju, A.-V. Phan, A. Pearsall, and S. Madanagopal, "Viscoelastic studies of human subscapularis tendon: Relaxation test and a Wiechert model," ***Computer Methods and Programs in Biomedicine***, 83(1): 29 - 33, (2006).

[12] J. Pacheco, C. Bavastri and J. Pereira, "Viscoelastic Relaxation Modulus Characterization Using Prony Series," ***Latin American Journal of Solids and Structures***, 12: 420-445, (2015).

[13] K. P. Menard and N. Menard, "Dynamic Mechanical Analysis," in ***Encyclopedia of Analytical Chemistry***, American Cancer Society, 1-25, (2017).

[14] M. C. Tanzi, S. Farè and G. Candiani, "Chapter 2 - Mechanical Properties of Materials," ***Foundations of Biomaterials Engineering***, Academic Press, (2019).

[15] A. Akinay, W. Brostow, V. Castano, R. Maksimov and P. Olszynski, "Time–temperature correspondence prediction of stress relaxation of polymeric materials from a minimum of data," ***Polymer***, 43: 3593-3600, (2002).

[16] E. A. Lopez-Guerra and S. d. J. Solares, "Modeling viscoelasticity through spring–dashpot models in intermittent-contact atomic force microscopy," ***Beilstein Journal of Nanotechnology***, 5: 2149 - 2163, (2014).

[17] J. Kim, H. Lee and N. Kim, "Determination of Shear and Bulk Moduli of Viscoelastic Solids from the Indirect Tension Creep Test," ***Journal of Engineering Mechanics-ASCE - J ENG MECH-ASCE***, 136(9): 1067-1075, (2010).

[18] https://www.mscsoftware.com/assets/103_elast_paper.pdf, MSC Software, "Nonlinear Finite Element Analysis of Elastomers from MSC software".

[19] N. Tschoegl and W. a. E. I. Knauss, "Poisson's Ratio in Linear Viscoelasticity – A Critical Review," ***Mechanics of Time-Dependent Material***, 6(1): 3-51, (2002).

[20] X. Wang, J. A. Schoen and M. E. Rentschler, "A quantitative comparison of soft tissue compressive viscoelastic model accuracy," ***Journal of the Mechanical Behavior of Biomedical Materials***, 20: 126 - 136, (2013).

[21] G. Basseri, M. Mehrabi Mazidi, F. Hosseini and M. K. Razavi Aghjeh, "Relationship among microstructure, linear viscoelastic behavior and mechanical properties of SBS triblock copolymer-compatibilized PP/SAN blend," ***Polymer Bulletin***, 71(2), (2013).

[22] https://www.doitpoms.ac.uk/tlplib/bioelasticity/viscoelasticity-hysteresis.php?printable=1, University of Cambridge, "Viscoelasticity and Hysteresis".

[23] K. Michalakis, P. L. Calvani and H. Hirayama, "Biomechanical considerations on tooth-implant supported fixed partial dentures," ***Journal of Dental Biomechanics***, 3, (2012).

[24] N. Özkaya, M. Nordin, D. Goldsheyder and D. Leger, "Mechanical Properties of Biological Tissues from BIOEN 520 of University of Washington," http://courses.washington.edu/bioen520/notes/Viscoelasticity.pdf (2012)

[25] Dunson, Debra L. “Characterization of Polymers using Dynamic Mechanical Analysis (DMA).” (2017).